Petroleum Research 6 (2021) 16–25

Contents lists available at ScienceDirect

Petroleum Research

journal homepage: http://www.keaipublishing.com/en/journals/petroleum-research/

Full Length Article

Investigating dynamic rock quality in two-phase flow systems using TEM-function: A comparative study of different rock typing indices

Mohsen Faramarzi-Palangar [a, d, *], Abouzar Mirzaei-Paiaman [b, c]

[a] Institute of Petroleum Engineering, School of Chemical Engineering, College of Engineering, University of Tehran, Tehran, Iran
[b] National Iranian South Oil Company (NISOC), Department of Petroleum Engineering, Ahvaz, Iran
[c] Now at State University of Campinas, São Paulo, Brazil
[d] Pars Petro Zagros (PPZ) Company, Tehran, Iran

ARTICLE INFO

Article history:
Received 13 June 2020
Received in revised form
14 August 2020
Accepted 14 August 2020
Available online 18 August 2020

Keywords:
TEM-function
Rock typing
Relative permeability
Capillary pressure
FZI-star

ABSTRACT

Constructing a reservoir simulation model requires an accurate definition of saturation functions, including capillary pressure and relative permeability data. Usually, these saturation functions are available only for a limited number of samples. Assigning saturation functions to the simulation model requires finding a clear relationship between them and a 3D predictable property of grid cells. Different indices are usually evaluated to describe such a relationship. It was recently shown that each petrophysical dynamic rock type should form similar True Effective Mobility (TEM) curves. In this study, TEM-function was used to evaluate the reliability and performance of different rock typing indices in defining dynamic rock types. FZI, FZIM, MFZI, and FZI* (FZI-star) indices were considered and tested on a collection of laboratory-derived core-flooding data from an Iranian carbonate reservoir. Results showed that FZI-star had a better performance than FZI, MFZI, and FZIM.

1. Introduction

Production optimization and reservoir performance predictions made by simulators require defining an accurate reservoir simulation model (Izadi and Ghalambor, 2013; Mirzaei-Paiaman et al., 2019b). Constructing an accurate reservoir simulation model requires an accurate grid cell model definition along with assigning reservoir properties such as saturation functions, including capillary pressure and relative permeability data. These functions that are measured in the special core analysis laboratory (SCAL) are usually available for a limited number of samples. Thus, assigning the saturation functions in static/dynamic models needs finding a clear relationship between a predictable 3D property of grid cells and these limited saturation function data (Mirzaei-Paiaman et al., 2019a). For achieving this purpose, rock typing as a key solution is used.

Conventionally, it was assuming that rocks within a particular rock type could be identified by similar capillary pressure and relative permeability curves (Ferreira et al., 2015; Izadi and Ghalambor, 2013; Mirzaei-Paiaman et al., 2015; Saboorian Jooybari et al., 2010). Rock typing was implementing based on similarity of primary drainage capillary pressure curves and then averaging these curves along with other saturation functions such as corresponding imbibition capillary pressure and relative permeability data in each group to input them collectively into a simulation model. However, Mirzaei-Paiaman et al. (2018) showed that rocks within a given rock type with similar primary drainage capillary pressure curves may establish scattered relative permeability curves and vice versa. Therefore, it has been shown that capillary pressure and relative permeability data should be classified by independent schemes, including static and dynamic rock typing (Mirzaei-Paiaman et al., 2018). A static rock type is defined as a set of rocks with similar capillary pressure curves, whereas a dynamic rock type is defined as a collection of rocks with similar fluid flow characteristics (Mirzaei-Paiaman et al., 2018). Mirzaei-Paiaman et al. (2019a) have shown independent schemes for static and dynamic rock typing using a significant amount of size and variety of data from a heterogeneous carbonate formation. Furthermore, Mirzaei-Paiaman et al. (2019b) have shown that the static and dynamic rock types exhibit significant differences in

* Corresponding author. Institute of Petroleum Engineering, School of Chemical Engineering, College of Engineering, University of Tehran, Tehran, Iran.
E-mail addresses: m.faramarzi@ut.ac.ir, mfaramarzi@parspetro.com (M. Faramarzi-Palangar), Mirzaei1986@gmail.com, Abouzar@unicamp.br (A. Mirzaei-Paiaman).

https://doi.org/10.1016/j.ptlrs.2020.08.001

many practical applications. Mirzaei-Paiaman et al. (2019b) also stated that the relative permeability data alone might be unable to verify the capability of rock typing indices. Thus, they presented a new technique of True Effective Mobility (TEM-function) as a robust and universal criterion for dynamic rock typing to reduce uncertainties in assigning the fluid flow saturation functions to grid cells of a simulation model. Mirzaei-paiaman et al. (2020) also used TEM-function for a carbonate reservoir to evaluate a new framework for pre-SCAL representative sample selection.

To characterize appropriate static and dynamic rock types, so far, various indices have been proposed from different perspectives. However, quantitative and core-based methods have been widely used. Mirzaei-Paiaman et al. (2018) classified the quantitative and core-based methods into different categories including permeability prediction models (Aguilera, 2002; Amaefule et al., 1993; Ghanbarian et al., 2019; Izadi and Ghalambor, 2013; Jaya et al., 2005; Kolodzie, 1980; Mirzaei-Paiaman et al., 2018, 2015; Nabawy et al., 2009; Ngo et al., 2015; Nooruddin and Hossain, 2011; Pittman, 1992; Rezaee et al., 2006, 2012), cut-off based methods (Rebelle, 2014), capillary pressure based models (Thomeer, 1960; Saboorian Jooybari et al., 2010; Xu and Torres-Verdín, 2013), and spontaneous imbibition rate-driven method of FZI** (FZI-double star (a modified flow zone indicator)) (Mirzaei-Paiaman and Saboorian-Jooybari, 2016). Among these, the permeability prediction models, including empirical and theoretical indices, are very popular. The empirical indices (Aguilera, 2002; Jaya et al., 2005; Kolodzie, 1980; Nabawy et al., 2009; Ngo et al., 2015; Pittman, 1992; Rezaee et al., 2006, 2012) correlate pore throat, porosity, and permeability using mercury injection capillary pressure (MICP) data. The use of empirical indices has several limitations, such as dependency on the data used for their development (Ghanbarian et al., 2019; Mirzaei-Paiaman et al., 2018). The theoretical indices such as FZI (flow zone indicator) and modified FZIs such as FZIM (Nooruddin and Hossain, 2011) and MFZI (Izadi and Ghalambor, 2013), RQI* (modified rock quality index) (Ferreira et al., 2015), and FZI* (FZI-star) (Mirzaei-Paiaman et al., 2018, 2015) are mainly based on the Kozeny-Carman (K–C) equation.

The mentioned indices are usually used to group rocks for further SCAL tests at routine core analysis (RCAL) stage. These indices are also evaluated for assigning saturation functions to simulation model grid cells. In this study, the aim is to check the performance and accuracy of different indices in the context of dynamic rock typing, by checking their ability to group TEM curves. By this work, the ability of different indices in establishing a clear relationship with the fluid flow properties is investigated. Such kind of verification is very important because such indices are usually used without proper verification studies.

2. Material and methods

2.1. Theoretical rock typing indices

Rock typing is an objective-dependent process. In other words, when the objective is assigning the capillary pressure data into simulation models, the static rock typing scheme should be used, whereas, when the aim is assigning the fluid flow characteristics, dynamic rock typing scheme needs to be employed (Mirzaei-Paiaman et al., 2018, 2019a; 2019b). In this regard, different rock typing indices are used to identify petrophysical dynamic rock types (PDRTs) and petrophysical static rock types PSRTs.

Mirzaei-Paiaman et al. (2018) proposed a PDRT index based on the original form of the K–C equation. Their index could also be derived from Darcy's law for single-phase flow. The original form of the K–C equation can be expressed as follows.

$$k = \varphi \frac{r_{mh}^2}{F_s \tau} \tag{1}$$

in which k (m^2) is the absolute permeability, φ (fraction) is the porosity, r_{mh} (m) is the effective or mean hydraulic unit radius, F_s (dimensionless) is the shape factor, and τ (dimensionless) is the hydraulic tortuosity. In Equation (1), $\frac{r_{mh}^2}{F_s \tau}$ represents geological attributes of sedimentary rocks and contains microstructural characteristics that regulate fluid flow (Mirzaei-Paiaman et al., 2018, 2019a). In this regard, Mirzaei-Paiaman et al. (2018) used $\frac{r_{mh}^2}{F_s \tau}$ as the correct flow zone indicator to generate the below equation:

$$FZI^* = 0.0314\sqrt{\frac{k}{\varphi}} = \frac{r_{mh}}{\sqrt{F_s \tau}} \tag{2}$$

in which porosity and permeability are in fraction and millidarcy (mD), and FZI* in μm is the correct flow zone indicator. Although this equation had already been proposed by Amaefule et al. (1993) as RQI in terms of the macroscopic petrophysical properties of a porous medium, Mirzaei-Paiaman et al. (2018) found RQI as a

Table 1
Rock and fluid data.

Sample ID	Permeability, k (mD)	Porosity, φ (%)	Irreducible water saturation, Swir (%)	Cementation factor, m (force fit, a = 1)	Water Viscosity, μ (cp)	Oil Viscosity, μ (cp)
1	0.82	19.67	26.54	2.17	1.4	0.88
2	3.64	20.36	11.5	2.15	1.18	1.03
3	0.64	14.45	12.92	1.82	1.18	1.03
4	9.24	21.35	12.69	2.12	1.18	1.03
5	6.51	19.74	16.1	1.98	1.18	1.03
6	7.41	19.18	22.95	1.84	1.4	0.88
7	9.24	17.89	29.88	2.19	1.18	1.03
8	6.12	14.61	17.66	2.25	1.18	1.03
9	6.77	15.13	20.61	2.33	1.18	1.03
10	16.76	18.18	23.77	2.48	1.18	1.03
11	186.77	22.81	17.41	2.09	1.4	0.88
12	333.7	26.33	23.88	2.37	1.18	1.03
13	19.27	15.19	26.38	2.39	1.18	1.03
14	3.54	11.01	30.68	2.21	1.18	1.03
15	94.06	16.68	6.22	2.18	1.4	0.88
16	1.17	7.84	23.08	2.12	1.4	0.88
17	983.48	24.25	14.39	2.19	1.4	0.88
18	1785.61	23.77	9.76	2.47	1.4	0.88

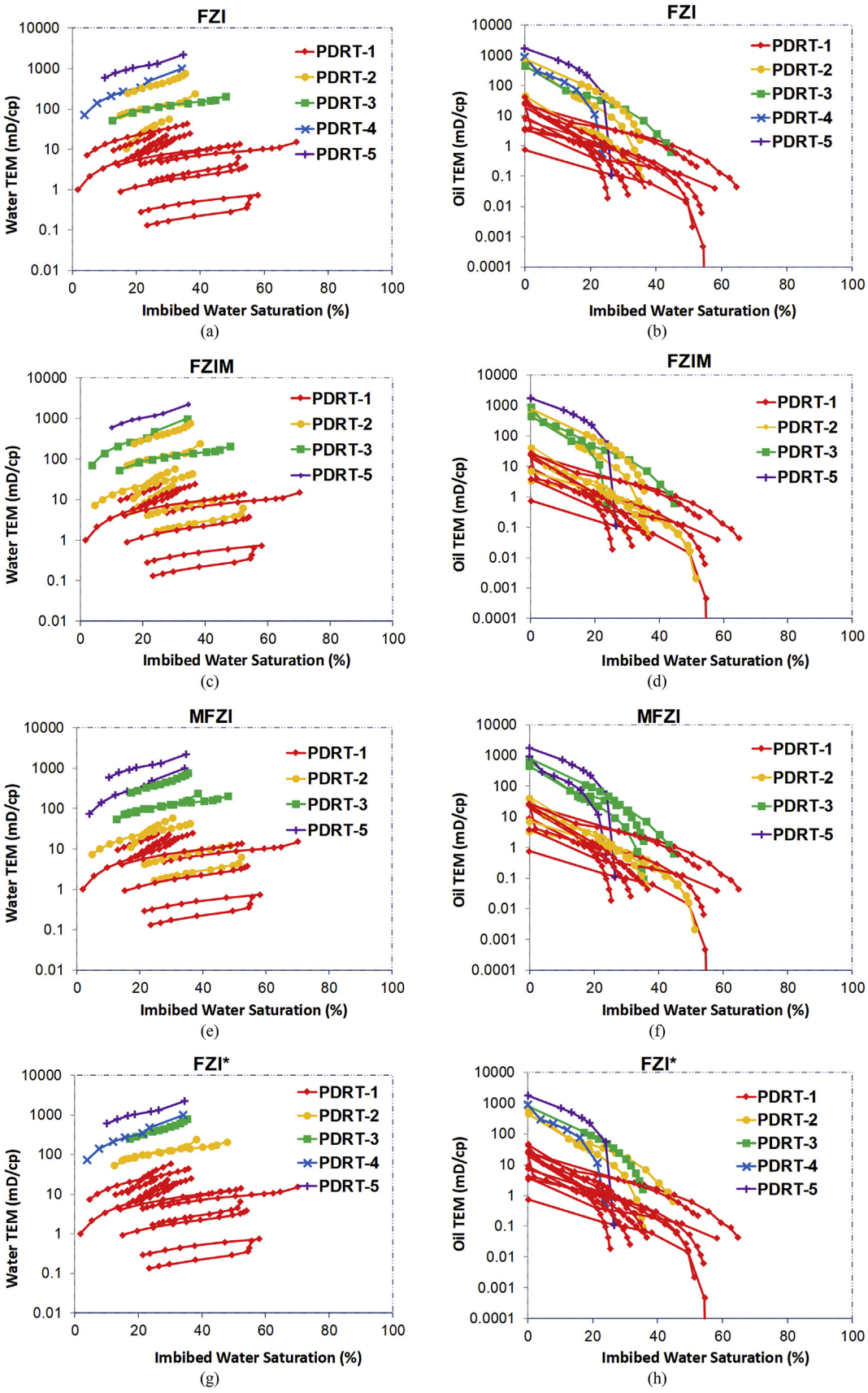

Fig. 1. Identification of PDRT using water-oil TEM data by FZI (a,b), FZIM (c,d), MFZI (e,f), and FZI* (g,h).

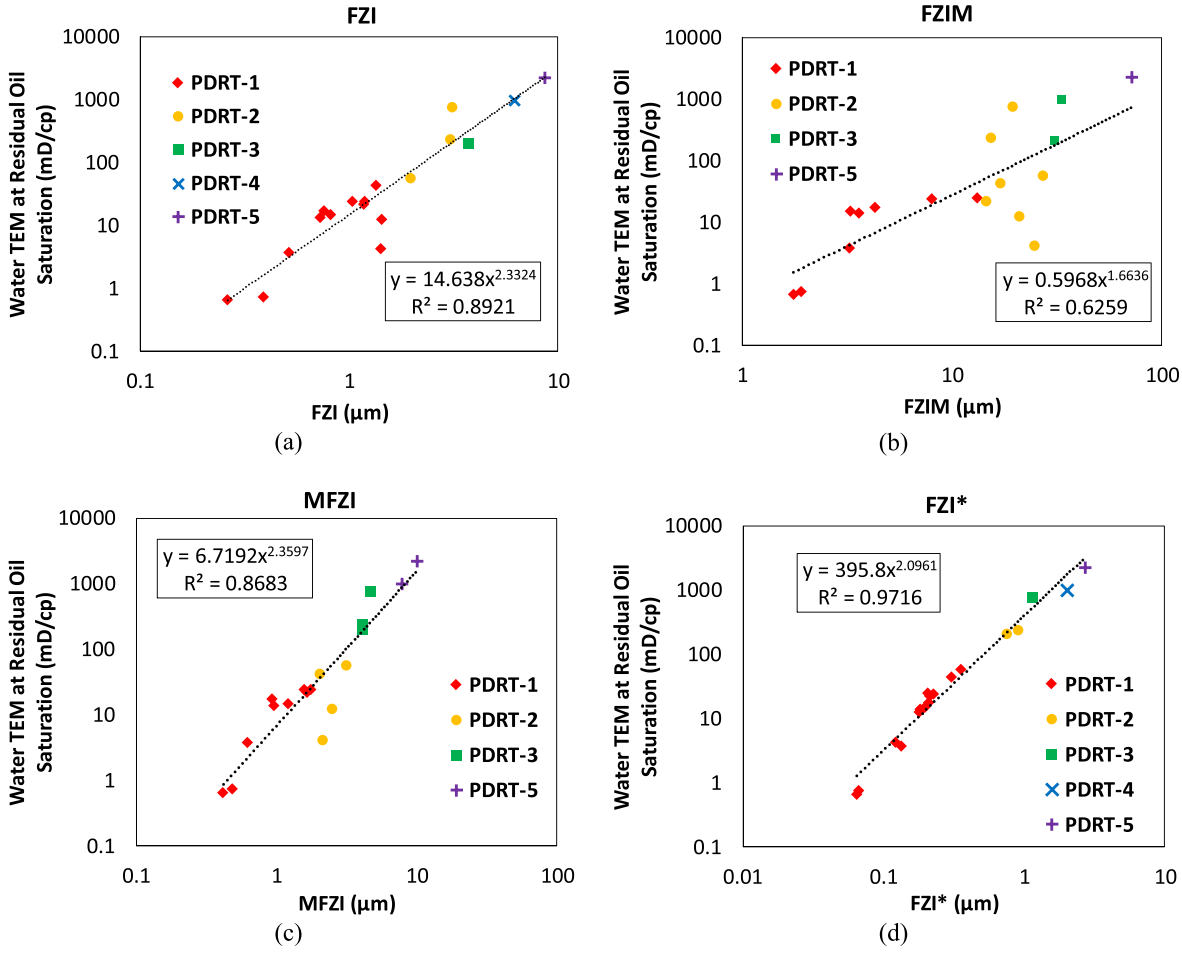

Fig. 2. The relationship between water TEM at residual oil saturation and (a) FZI, (b) FZIM, (c) MFZI, and (d) FZI*.

correct flow zone indicator and named it FZI*. Samples with similar FZI* values show similar fluid flow or dynamic behavior and form a particular PDRT or core-scale single-phase hydraulic flow unit (HFU). For a PDRT, cross-plot of $0.0314\sqrt{k}$ vs. $\sqrt{\varphi}$ on the log-log scale yields a unit-slope straight line where the average FZI* of each rock type can be determined from the intercept of this line at $\varphi = 1$. Samples with different FZI* should appear as a series of parallel lines on a logarithmic scale.

Mirzaei-Paiaman et al. (2018) also developed a PSRT index by coupling Young-Laplace equation for capillary pressure and the original form of the K–C equation, as follows:

$$PSRTI = 0.0314\sqrt{\frac{k}{\varphi}F_s\tau} = FZI^*\sqrt{F_s\tau} \tag{3}$$

where PSRTI in µm is the PSRT indicator. Mirzaei-Paiaman et al. (2018) stated that samples with similar PSRTI values show similar primary drainage capillary pressure curves and form a particular PSRT. However, is a parameter that cannot be easily measured for each rock sample, individually. In this regard, Mirzaei-Paiaman et al. (2018) suggested that FZI* becomes the only available and practical index for defining PSRTs. However, the accuracy of identifying PSRTs depends on the complexity of pore structures of considered rocks.

Other theoretical rock typing indices have been derived from the general form of the K–C equation (Carman, 1937; Kozeny, 1927). The general form of the K–C equation can be written as follow:

$$k = \frac{\varphi^3}{(1-\varphi)^2}\left(\frac{1}{F_s\tau S_{gv}^2}\right) \tag{4}$$

where S_{gv} (1/m) is the surface area per unit grain volume. Amaefule et al. (1993), as pioneers, based on the general form of the K–C equation, proposed a technique to classify reservoir rock into distinct petrophysical rock types. Amaefule et al. (1993) defined FZI as:

$$FZI = \frac{RQI}{\varphi_z} = \frac{1}{S_{gv}\sqrt{F_s\tau}} \tag{5}$$

where RQI is the rock quality index, and φ_z is the normalized porosity. Amaefule et al. (1993) stated that the rocks with similar FZI values show similar pore throat attributes and form a particular rock type. However, in terms of microscopic properties of a porous medium, FZI is a function of S_{gv} showing a grain size attribute or solid component which is not interested in fluid flow (Mirzaei-Paiaman et al., 2018).

Nooruddin and Hossain (2011) proposed another index based on a modification of the general form of the K–C equation by handling the tortuosity term as:

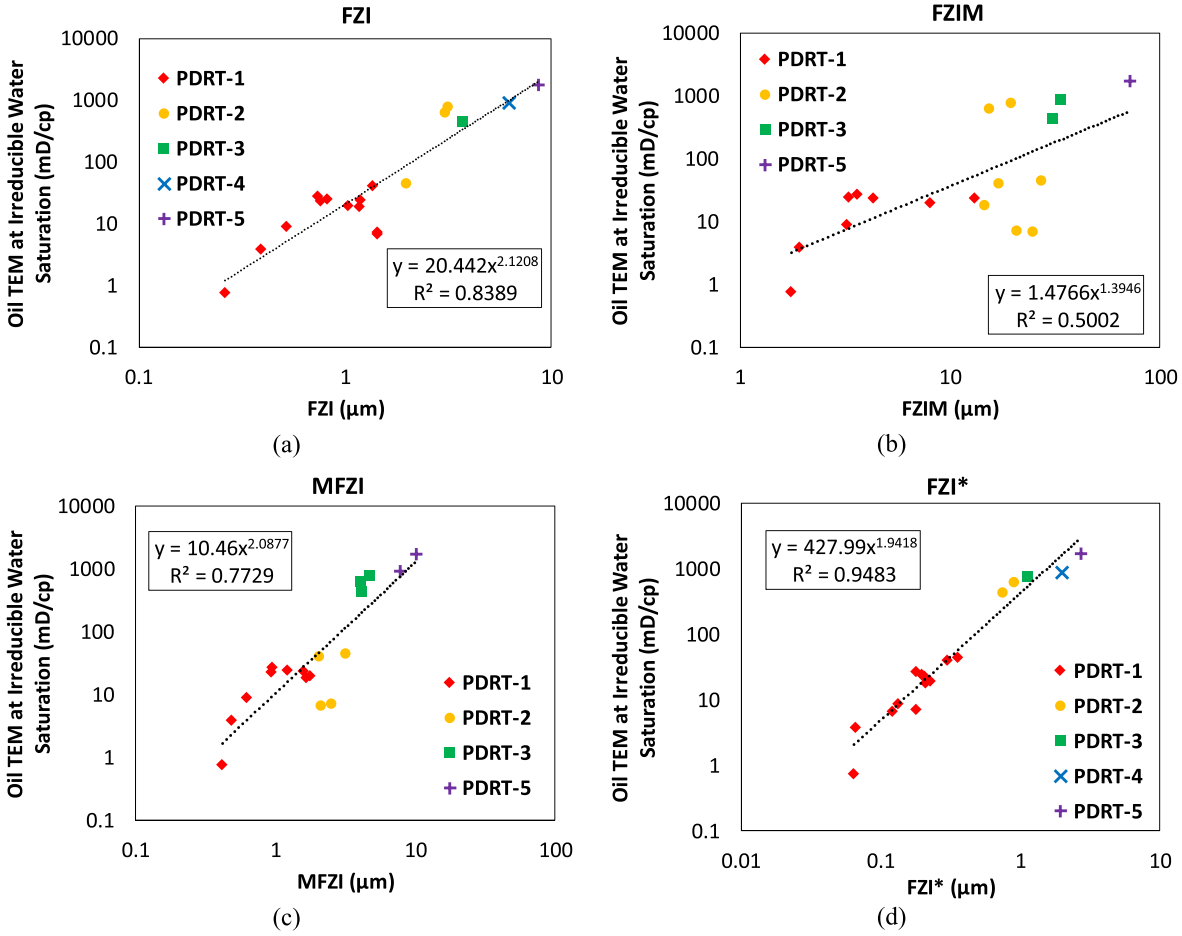

Fig. 3. The relationship between oil TEM at irreducible water saturation and (a) FZI, (b) FZIM, (c) MFZI, and (d) FZI*.

$$FZIM = \frac{RQI}{\varphi^{m-1}\varphi_z} = \frac{1}{\sqrt{F_s a^2 S_{gv}^2}} \tag{6}$$

where FZIM (m) is a modified flow zone indicator, m (dimensionless) is the cementation factor, and *a* (dimensionless) is the tortuosity factor. Nooruddin and Hossain (2011) did not verify their index using SCAL data. In the work conducted by Nooruddin and Hossain (2011), electrical tortuosity has been considered improperly instead of hydraulic tortuosity, whereas electrical and hydraulic tortuosity have physical and conceptual differences (Ghanbarian et al., 2013; Mirzaei-Paiaman et al., 2018, 2015; Soleymanzadeh et al., 2018). Besides, since Nooruddin and Hossain (2011) inappropriately substituted the tortuosity term in the general form of the K–C equation, the governing factors of the rock texture have been excluded from the FZI (Mirzaei-Paiaman et al., 2015). It means that FZIM not only does not improve the FZI model, but also undermines it. Moreover, dependency of FZIM to cementation factor makes it difficult to use (Mirzaei-Paiaman et al., 2015).

Izadi and Ghalambor (2013) developed a modified index from the general form of K–C equation by considering the irreducible water saturation as an additional parameter, as:

$$MFZI = \frac{RQI}{\varphi_z(1 - S_{wir})^{1.5}} = \frac{1}{\sqrt{F_s \tau S_{gv}^2}} \tag{7}$$

in which MFZI (m) is a modified flow zone indicator, and S_{wir} (fraction) is the irreducible water saturation. In the work conducted by Izadi and Ghalambor (2013), S_{wir} is a function of wettability which may adversely affect identifying petrophysical rock types (Mirzaei-Paiaman et al., 2015).

FZI (Amaefule et al., 1993), FZIM (Nooruddin and Hossain, 2011), and MFZI (Izadi and Ghalambor, 2013) all are based on the generalized form of the K–C equation whereas the FZI* is based on the basic or original form of the K–C equation (Mirzaei-Paiaman et al., 2018, 2015). In terms of microstructure characteristics, the methods that are based on the generalized form of the K–C equation are a function of the grain size (i.e., S_{gv}), which is not interested in the dynamic behavior of a system. However, FZI* is a function of the effective or mean hydraulic radius, which is an effective parameter in fluid flow through the porous medium. In other words, the pore properties of a porous system are more interested in fluid flow and dynamic behavior than the solid component properties (Mirzaei-Paiaman et al., 2018). Furthermore, Amaefule et al. (1993), Nooruddin and Hossain (2011), and Izadi and Ghalambor (2013) have not defined the objectives of their indices, either for static, or dynamic rock typing. In other words, FZI, FZIM, and MFZI are not able to discriminate between PDRTs and PSRTs (Mirzaei-Paiaman et al., 2018, 2019a). Moreover, the use of FZIM (Nooruddin and

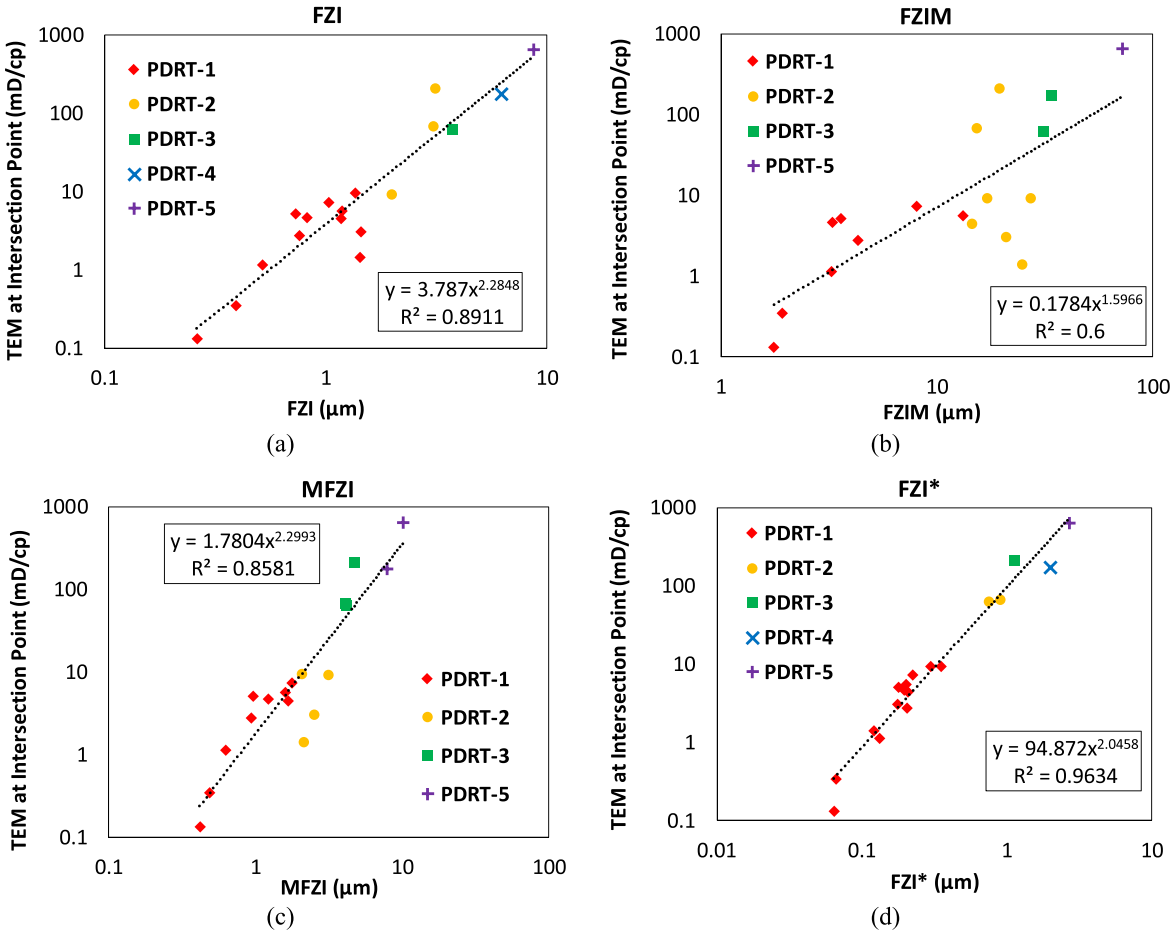

Fig. 4. The relationship between TEM at intersection point and (a) FZI, (b) FZIM, (c) MFZI, and (d) FZI*.

Hossain, 2011) and MFZI (Izadi and Ghalambor, 2013) needs prior knowledge of some kind of SCAL data (Mirzaei-Paiaman et al., 2018, 2019a). The use of these two indices is challenging in further sample selection for SCAL test at RCAL stage. Ultimately, FZI, MFZI and FZIM have not been checked using an appropriate verification method. Thus, it is essential to check and verify the accuracy and performance of each index using SCAL data.

2.2. TEM function

It has been historically considered that rocks within a PDRT should show similar relative permeability curves. In practice, establishing a robust relationship between PDRTs and relative permeability data is more challenging (Mirzaei-Paiaman et al., 2018). In this regard, Mirzaei-Paiaman et al. (2019b) recently proposed a criterion named TEM-function for characterizing dynamic rock quality in multiphase flow applications as:

$$TEM_\alpha = \frac{kk_{ra}}{\varphi\mu_\alpha} = -\frac{\upsilon_\alpha}{\nabla p_\alpha} \tag{8}$$

where k_r (fraction) is the relative permeability, μ (Pa.s) is the fluid viscosity, υ (m/s) is the fluid or interstitial velocity, ∇p (Pa/m) is the pressure gradient, and α represents a fluid phase. The ratio of $\frac{\upsilon_\alpha}{\nabla p_\alpha}$ indicates the capability of a porous medium in fluid flow under a particular pressure gradient. In a particular pressure gradient, systems, or rocks with higher fluid velocity exhibit more efficient in the permission of fluid flow than low fluid velocity. Furthermore, systems with the same fluid flow behavior or same PDRT form similar TEM curves. Moreover, those systems exhibiting higher fluid flow efficiency place above the curves of less efficient ones (Mirzaei-Paiaman et al., 2019b).

However, Darcy's law may not be accurate in some certain reservoirs, such as very tight reservoirs (Fuquan et al., 2019; Govindarajan, 2019; Hailong, 2017; Yao and Ge, 2011). Thus, TEM-function in such cases should be used with caution.

2.3. Data collection

The under-study reservoir is a shallow marine Iranian carbonate formation in Neocomian age. Depositional facies are mainly composed of shoal and lower shoal facies. It is a massive oolitic to pellety limestone with minor contemporaneous brecciation in the basal part at the type section. The studied reservoir consists of zones X-1, X-2, X-3, and X-4.

- **X-1**: It is characterized by the deposition of gray packstone/wackestone in a medium-low energy depositional environment. Developed horizontal fractures and open fractures contain oil that can be observed in local cores.
- **X-2**: The core component is mainly packstone and wackestone, which represents a medium-low energy depositional

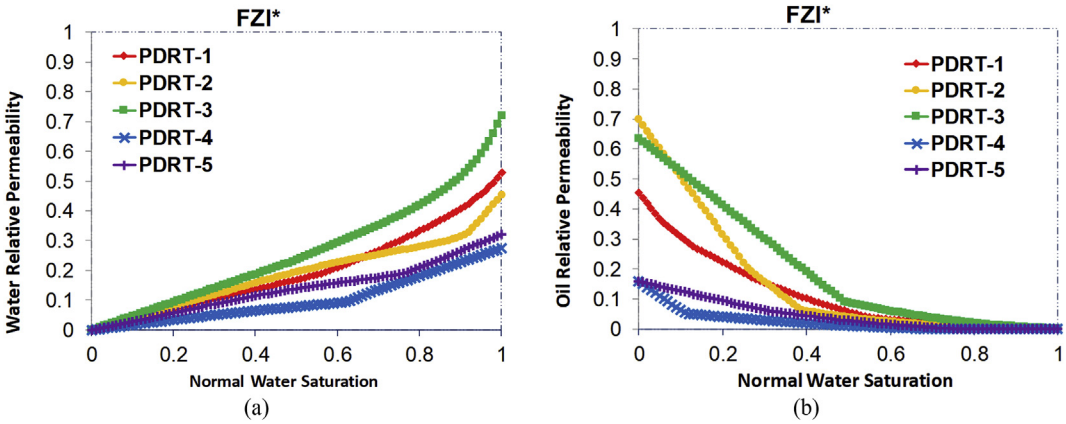

Fig. 5. Average relative permeability using Equation (1) for the PDRTs identified by FZI* method: (a) water (b) oil.

environment. The cores are wrapped with light crude oil, and are homogenous and have good oil shows. They are with visible dissolution pores.

- **X-3**: The component of core is mainly blocky packstone and wackestone, which represents a medium-low energy depositional environment. The oil-bearing cores show dark color and make a sharp contrast with the tight surrounding gray rock, which showed heterogeneity. The component of cores is tight, and the oil saturation is low.
- **X-4**: The component of core is mainly blocky packstone and wackestone, which represents a medium-high energy depositional environment. The oil-bearing cores show a dark color with high oil saturation.

SCAL data (i.e., water-oil primary imbibition relative permeability, water-oil primary drainage capillary pressure, force imbibition capillary pressure, secondary drainage capillary pressure, and formation resistivity factor) along with routine data (porosity and permeability) were collected from this carbonate reservoir at SW of Iran, NW Persian Gulf. Table 1 shows the rock and fluids data. The wettability of our samples was assessed using Craig's rules of thumb, Amott, and Amott-Harvey index (Amott, 1959; Anderson, 1986a,b, 1987a,b,c; Craig, 1971). Results are displayed in the **Appendix**. Wettability analysis shows that the wettability of the studied reservoir is oil-wet. It is noteworthy to mention that several other wettability indices have been proposed in the literature, for example relative pseudo work of imbibition (Ma et al., 1999) and MPMS (Mirzaei-Paiaman et al., 2013, 2017). In this study, we did not have access to the required data to run those methods.

3. Results and discussion

In this section, performance of different indices in defining the PDRTs was compared using the TEM technique. To identify PDRTs, the value of an index for each sample was calculated. Then, the difference between maximum and minimum values for each index was divided into five groups with equal division to compare the results. In following, PDRT 1 is marked red, PDRT 2 orange, PDRT 3 green, PDRT 4 blue, and PDRT 5 purple.

In our analysis, we plot TEM data versus the imbibed water saturation ($S_w - S_{wir}$) defined as the difference between water saturation and irreducible water saturation. Using the imbibed water saturation on the horizontal axis causes that all curves start from a common point of zero. This is a necessary condition to compare the TEM curves. Fig. 1 shows the PDRTs predicted by different indices. An appropriate rock typing index should be able to give separate and distinct PDRTs. FZI, FZIM, and MFZI show some overlap in water TEM curves, whereas water TEM curves are well-separated using FZI*. Although FZI* well-separated water TEM curves, some overlapping still exists in oil TEM curves.

Fig. 2 indicates the relationship between water TEM at residual oil saturation and different indices. FZI* showed a strong correlation with water TEM at residual oil saturation with R^2 of 0.97, followed by FZI with R^2 of 0.89, MFZI with R^2 of 0.87, and FZIM with R^2 of 0.63. Fig. 3 depicts the relationship between oil TEM at irreducible water saturation and different indices. FZI*, FZI, MFZI, and FZIM each made R^2 values of 0.95, 0.84, 0.77, and 0.50, respectively. The results confirm the performance and superiority of FZI* in comparison with FZI, FZIM, and MFZI. Fig. 4 also illustrates the relationship between the indices and TEM at the intersection point of TEM curves, where oil and water TEMs are equal. FZI* and FZI gave the highest R^2 values of 0.96 and 0.89, respectively, whereas R^2 of MFZI and FZIM was 0.86 and 0.60, respectively.

FZI* with the best correlation coefficients represents an accurate index in defining the PDRTs in this reservoir. The good performance of FZI* in establishing strong correlation with endpoint and crossover TEMs is because the TEM already has $\frac{k}{\varphi}$ inside. In fact, dependency of TEM on $\frac{k}{\varphi}$ leads to such high R^2 values. This shows that rock quality in single- and two-phase systems are to some degrees interrelated.

It is noteworthy that FZI gives better results than FZIM and MFZI, whereas these indices have been introduced as a modified FZI and bear complex parameters. It can be concluded that adding complex parameters not only makes the problem more complex, but also reduces the performance and accuracy of indices in defining the PDRTs.

A common method for assigning the saturation functions into simulators is the use of average saturation function of each group. Mirzaei-Paiaman et al. (2019b) proposed an equation for averaging relative permeability curves in a PDRT as:

$$\overline{k_{r\alpha}} = \frac{\sum_{i=1}^{n} TEM_{i\alpha}}{\sum_{i=1}^{n}\left(\frac{k}{\mu\varphi}\right)_i} = \frac{\sum_{i=1}^{n}\left(\frac{kk_{\alpha}}{\mu\varphi}\right)_i}{\sum_{i=1}^{n}\left(\frac{k}{\mu\varphi}\right)_i} \tag{9}$$

Fig. 5 shows the average relative permeability curves of water and oil using this equation. The average relative permeability

curves have an interesting point. Average relative permeability curves of lower quality PDRTs sometimes are observed above the curves for higher quality PDRTs. It well shows that relative permeability alone is not suitable for studying the dynamic behavior of rocks, and TEM should be used instead.

4. Conclusions

In this study, the performance and accuracy of different rock typing indices in studying petrophysical dynamic rock types was checked using the TEM-function. The conclusions of this work can be drawn as:

- Among the indices checked, FZI* had the highest accuracy and best performance in identifying dynamic rock types and separation of TEM curves.
- Adding the complex parameters to rock typing indices not only does not improve them, but may also undermine their applicability.
- The relative permeability curves of a rock with higher fluid flow quality sometimes may fall below the curves of a lower quality system. It indicates that relative permeability alone is not suitable for studying the dynamic behavior of rocks, and TEM should be used instead.

Appendix

Craig's rules of thumb (Craig, 1971), Amott, (1959), Amott-Harvey (Amott, 1959) and capillary pressure curves were used to determine the type of wettability for this reservoir.

Table 2-A shows Craig's rules of thumb. Table 3-A indicates the wettability state of each sample identified by each Craig's rule. Craig's first rule of thumb indicates that most samples are oil-wet. Oil wetness is concluded for all samples by the second rule of Craig. Craig's third rule gives contradictory predictions to the first and second rules. In general, we found Craig's rules contradictory to each other. Investigating the limitations of Craig's rules is worthy for future research.

Table 4-A describes wettability evaluation from Amott and Amott-Harvey methods. Fig. 6-A illustrates the available primary drainage, forced imbibition, and secondary forced drainage capillary pressure data for the studied reservoir. Based on capillary pressure data the samples are oil-wet. For a different set of samples from this reservoir, Amott-Harvey index analysis is available (see Table 5-A). Results indicate that the wettability of these samples is oil-wet. In conclusion, the wetness of the studied reservoir is oil-wet.

Table 2-A
Craig's rules of thumb (Craig, 1971; Anderson, 1987b).

Craig's rules	Criterion	Water-Wet	Oil-Wet
First rule	Water relative permeability at residual oil saturation; based on the oil permeability at irreducible water saturation.	Generally less than 30%	Greater than 50% and approaching 100%
Second rule	Water saturation at crossover point of relative permeability curves	Greater than 50% water saturation	Less than 50% water saturation
Third rule	Irreducible water saturation	Usually greater than 20 to 20% pore volume	Generally less than 15% pore volume

Table 3-A
Results of wettability determination using Craig's rules of thumb.

Sample ID	Water relative permeability at residual oil saturation	Water saturation at crossover point of relative permeability curves	Irreducible water saturation
1	0.22	0.42	26.54
2	0.25	0.35	11.5
3	0.2	0.44	12.92
4	0.47	0.23	12.69
5	0.49	0.35	16.1
6	0.54	0.38	22.95
7	0.55	0.39	29.88
8	0.69	0.43	17.66
9	0.59	0.48	20.61
10	0.56	0.18	23.77
11	0.41	0.38	17.41
12	0.72	0.42	23.88
13	0.54	0.48	26.38
14	0.46	0.32	30.68
15	0.52	0.31	6.22
16	0.59	0.4	23.08
17	0.28	0.27	14.39
18	0.32	0.31	9.76

Table 4-A
The relationship between the wettability and Amott and Amott-Harvey methods.

Wettability index	Description	Water-Wet	Neutrally Wet	Oil-Wet
Amott	I_w: Displacement-by-water ratio	Positive	Zero	Zero
	I_o: Displacement-by-oil ratio	Zero	Zero	Positive
Amott-Harvey	$I_w - I_o$	$0.3 \leq WI \leq 1.0$	$-0.3 < WI < 0.3$	$-1.0 \leq WI \leq -0.3$

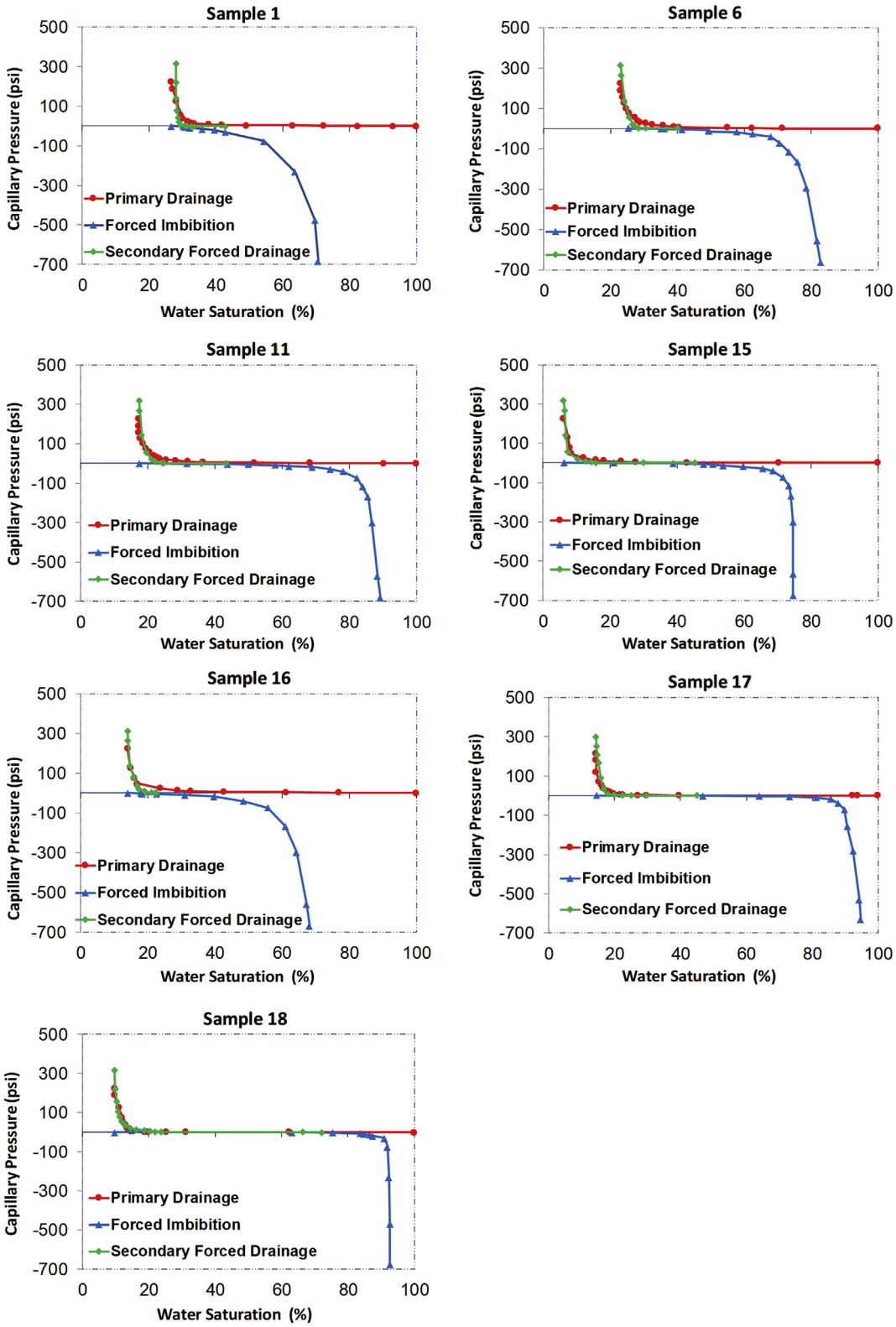

Fig. 6-A. Primary drainage, forced imbibition, and secondary forced drainage capillary pressure data.

Table 5-A
Wettability measurement using Amott-Harvey Index.

Sample ID	Irreducible water saturation (%)	Porosity (%)	Air permeability (mD)	Water Wettability Index, (Iw)	Oil Wettability Index, (Io)	Amott-Harvey wettability Index, (WI=Iw-Io)
19	8.20	14.54	12.895	0.027	0.500	−0.473
20	29.16	20.52	17.066	0.000	0.639	−0.639
21	36.63	12.56	5.299	0.009	0.549	−0.540
22	29.66	15.48	12.319	0.000	0.756	−0.756
23	10.86	16.74	1.386	0.005	0.226	−0.221
24	32.60	20.44	8.248	0.009	0.380	−0.371
25	16.30	17.14	3.553	0.009	0.459	−0.450

References

Aguilera, R., 2002. Incorporating capillary pressure, pore throat aperture radii, height above free-water table, and Winland r35 values on Pickett plots. AAPG Bull. 86 (4), 605–624.

Amaefule, J.O., Altunbay, M., Tiab, D., Kersey, D.G., Keelan, D.K., 1993. Enhanced reservoir description: using core and log data to identify hydraulic (flow) units and predict permeability in uncored intervals/wells. SPE Annu. Tech. Conf. Exhib. https://doi.org/10.2118/26436-MS.

Amott, E., 1959. Observations relating to the wettability of porous rock. Transactions of the AIME 216 (1), 156–162.

Anderson, W.G., 1986a. Wettability literature survey – Part 1: rock/oil/brine interactions and the effects of core handling on wettability. J. Petrol. Technol. 38, 1125–1145.

Anderson, W.G., 1986b. Wettability literature survey – Part 2: wettability measurement. J. Petrol. Technol. 38, 1246–1262. https://doi.org/10.2118/13933-pa.

Anderson, W.G., 1987a. Wettability literature survey – Part 4: effects of wettability on capillary pressure. Paper SPE-15271. J. Petrol. Technol. 39 (10), 1283–1300. https://doi.org/10.2118/15271-PA.

Anderson, W.G., 1987b. Wettability literature survey – Part 5: the effects of wettability on relative permeability. Paper SPE-16323. J. Petrol. Technol. 39 (11), 1453–1468. https://doi.org/10.2118/16323-PA.

Anderson, W.G., 1987c. Wettability literature survey – Part 6: the effects of wettability on waterflooding. J. Petrol. Technol. 39, 1605–1622. https://doi.org/10.1016/0148-9062(88)91583-5.

Carman, P.C., 1937. Fluid flow through granular beds. Trans. Inst. Chem. Eng. 15, 150–166. https://doi.org/10.1016/S0263-8762(97)80003-2.

Craig, F.F., 1971. The Reservoir Engineering Aspects of Waterflooding, vol. 3. HL Doherty Memorial Fund of AIME, New York, pp. 12–44.

Ferreira, A.F.C., Wahanik, H., Booth, R., Carneiro, G., Bize-forest, N., Oliveira, R., 2015. New Rock-Typing Index Based on Hydraulic and Electric Tortuosity Data for Multi-Scale Dynamic Characterization of Complex Carbonate Reservoirs 1. https://doi.org/10.2118/175014-MS.

Fuquan, S., Xingxing, S., Yong, W., Yeheng, S., 2019. Single- and two-phase flow model in low-permeability reservoir. Petroleum 5, 183–190. https://doi.org/10.1016/j.petlm.2018.05.004.

Ghanbarian, B., Hunt, A.G., Ewing, R.P., Sahimi, M., 2013. Tortuosity in porous media: a critical review. Soil Sci. Soc. Am. J. 77, 1461. https://doi.org/10.2136/sssaj2012.0435.

Ghanbarian, B., Lake, L.W., Sahimi, M., 2019. Insights into rock typing: a critical study. SPE J. 24 (1), 230–242. https://doi.org/10.2118/191366-PA.

Govindarajan, S.K., 2019. An overview on extension and limitations of macroscopic Darcy's law for a single and multi-phase fluid flow through a porous medium. Int. J. Min. Sci 5. https://doi.org/10.20431/2454-9460.0504001.

Hailong, L., 2017. The numerical simulation for multistage fractured horizontal well in low-permeability reservoirs based on modified Darcy's equation. J. Pet. Explor. Prod. Technol 7, 735–746. https://doi.org/10.1007/s13202-016-0283-1.

Izadi, M., Ghalambor, A., 2013. New approach in permeability and hydraulic-flow-unit determination. SPE Reservoir Eval. Eng. 16, 257–264. https://doi.org/10.2118/151576-PA.

Jaya, I., Sudaryanto, A., Widarsono, B., 2005. Permeability prediction using pore throat and rock fabric: a model from Indonesian reservoirs. Proc. SPE Asia Pacific Oil Gas Conf. Exhib. https://doi.org/10.2523/93363-MS.

Kolodzie, S., 1980. Analysis of pore throat size and use of the Waxman-Smits equation to determine OOIP in Spindle field. In: Colorado. SPE-9382-MS, SPE Annual Technical Conference and Exhibition, 21–24 September. https://doi.org/10.2118/9382-ms. Dallas, Texas.

Kozeny, J., 1927. Ber kapillare Leitung des Wassers im Boden, Sitzungsberichte. Royal Academy of Science Vienna. Proc. Cl. I 136, 271–306.

Ma, S., Morrow, N.R., Zhou, X., 1999. Characterization of wettability from spontaneous imbibition measurements. J Can Pet Technol Special Edition 38 (13), 1–8.

Mirzaei-Paiaman, A., Masihi, M., Standnes, D.C., 2013. Index for characterizing wettability of reservoir rocks based on spontaneous imbibition recovery data. Energy Fuels 27 (12), 7360–7368.

Mirzaei-Paiaman, A., Ostadhassan, M., Rezaee, R., Saboorian-Jooybari, H., Chen, Z., 2018. A new approach in petrophysical rock typing. J. Petrol. Sci. Eng. 166, 445–464. https://doi.org/10.1016/j.petrol.2018.03.075.

Mirzaei-paiaman, A., Reza, S., Saboorian-jooybari, H., 2020. A new framework for selection of representative samples for special core analysis. Pet. Res. https://doi.org/10.1016/j.ptlrs.2020.06.003.

Mirzaei-Paiaman, A., Saboorian-Jooybari, H., 2016. A method based on spontaneous imbibition for characterization of pore structure: application in pre-SCAL sample selection and rock typing. J. Nat. Gas Sci. Eng. 35, 814–825. https://doi.org/10.1016/j.jngse.2016.09.023.

Mirzaei-Paiaman, A., Sabbagh, F., Ostadhassan, M., Shafiei, A., Rezaee, R., Saboorian-Jooybari, H., Chen, Z., 2019a. A further verification of FZI* and PSRTI: newly developed petrophysical rock typing indices. J. Petrol. Sci. Eng. 175, 693–705. https://doi.org/10.1016/j.petrol.2019.01.014.

Mirzaei-Paiaman, A., Saboorian-Jooybari, H., Chen, Z., Ostadhassan, M., 2019b. New technique of True Effective Mobility (TEM-Function) in dynamic rock typing: reduction of uncertainties in relative permeability data for reservoir simulation. J. Petrol. Sci. Eng. 179, 210–227. https://doi.org/10.1016/j.petrol.2019.04.044.

Mirzaei-Paiaman, A., Saboorian-Jooybari, H., Masihi, M., 2017. Incorporation of viscosity scaling group into analysis of MPMS index for laboratory characterization of wettability of reservoir rocks. J. Pet. Explor. Prod. Technol 7 (1), 205–216.

Mirzaei-Paiaman, A., Saboorian-Jooybari, H., Pourafshary, P., 2015. Improved method to identify hydraulic flow units for reservoir characterization. Energy Technol. 3, 726–733. https://doi.org/10.1002/ente.201500010.

Nabawy, B.S., Géraud, Y., Rochette, P., Bur, N., 2009. Pore-throat characterization in highly porous and permeable sandstones. Am. Assoc. Petrol. Geol. Bull. 93, 719–739. https://doi.org/10.1306/03160908131.

Ngo, V.T., Lu, V.D., Nguyen, M.H., Hoang, T.M., Nguyen, H.M., Le, V.M., 2015. A comparison of permeability prediction methods using core analysis data. SPE Reserv. Characterisation Simul. Conf. Exhib. https://doi.org/10.2118/175650-MS.

Nooruddin, H.A., Hossain, M.E., 2011. Modified Kozeny-Carmen correlation for enhanced hydraulic flow unit characterization. J. Petrol. Sci. Eng. 80, 107–115. https://doi.org/10.1016/j.petrol.2011.11.003.

Pittman, E.D., 1992. Relationship of porosity and permeability to various parameters derived from mercury injection capillary pressure curves for sandstones. AAPG Bull. 76 (2), 191–198.

Rebelle, M., 2014. Rock-typing in carbonates: a critical review of clustering methods. Abu Dhabi Int. Pet. Exhib. Conf 14. https://doi.org/10.2118/171759-MS.

Rezaee, M.R., Jafari, A., Kazemzadeh, E., 2006. Relationships between permeability, porosity and pore throat size in carbonate rocks using regression analysis and neural networks. J. Geophys. Eng. 3, 370–376. https://doi.org/10.1088/1742-2132/3/4/008.

Rezaee, R., Saeedi, A., Clennell, B., 2012. Tight gas sands permeability estimation from mercury injection capillary pressure and nuclear magnetic resonance data. J. Petrol. Sci. Eng. 88–89, 92–99. https://doi.org/10.1016/j.petrol.2011.12.014.

Saboorian Jooybari, H., Movazi, G.H., Jaberi, R., 2010. A new approach for rock typing used in one of the Iranian carbonate reservoir (a case study). Int. Oil Gas Conf. Exhib. China.

Soleymanzadeh, A., Jamialahmadi, M., Helalizadeh, A., Soulgani, B.S., 2018. A new technique for electrical rock typing and estimation of cementation factor in carbonate rocks. J. Petrol. Sci. Eng. 166, 381–388. https://doi.org/10.1016/j.petrol.2018.03.045.

Thomeer, J.H.M., 1960. Introduction of a pore geometrical factor defined by the capillary pressure curve. SPE-1324-G J. Pet. Technol 12 (3), 73–77. https://doi.org/10.2118/1324-G.

Xu, C., Torres-Verdín, C., 2013. Pore system characterization and petrophysical rock classification using a bimodal Gaussian density function. Math. Geosci. 45 (6), 753–771. https://doi.org/10.1007/s11004-013-9473-2.

Yao, Y., Ge, J., 2011. Characteristics of non-Darcy flow in low-permeability reservoirs. Petrol. Sci. 8, 55–62. https://doi.org/10.1007/s12182-011-0115-3.